RAA 2021 Vol. **21** No. **10**, 244(10pp) doi: 10.1088/1674-4527/21/10/244

http://www.raa-journal.org *http://iopscience.iop.org/raa*

Research in Astronomy and Astrophysics

New design of large fully-steerable radio telescope reflector based on homogenized mesh structure

Li-De Yan, Fei Zheng and Xi Rui

School of Mechano-Electronic Engineering, Xidian University, Xi'an 710071, China; *yanlide2021@163.com*

Received 2021 March 11; accepted 2021 May 5

Abstract The self-weight of a large fully-steerable radio telescope is one of the important factors affecting its performance. In the existing reflector system scheme, the problem of surface accuracy caused by its large and heavy structure has seriously restricted the application and implementation of large radio telescopes. Therefore, a new mesh structure scheme for a large fully-steerable radio telescope reflector is proposed in this paper. This scheme is based on a homogenized mesh back-up structure in the form of a quasi-geodesic grid and regular quasi-tri-prism or tetrahedron, which can significantly reduce the structural complexity and self-weight of the reflector under the condition that the reflector can meet the desired performance requirements. Finally, the feasibility and rationality of the scheme are evaluated by numerical simulation analysis, which has significant advantages and provides a new design for the reflector of a large fully-steerable radio telescope.

Key words: telescopes — techniques: radar astronomy — methods: data analysis

1 INTRODUCTION

A large fully-steerable radio telescope is a precision instrument mainly used for receiving faint electromagnetic radiation. Its characteristics of large aperture, high gain, narrow beam, high resolution and high sensitivity are of great significance for detecting extraterrestrial civilization, expanding human cognition and enhancing international influence (Cheng 2009; Hao et al. 2010; Zhang et al. 2019). In the field of radio astronomy in China, the Five-hundred-meter Aperture Spherical radio Telescope (FAST) facility (Nan 2005; Gan & Jin 2010) and the planned Qitai Telescope (QTT) with a 110 m diameter (Xu & Wang 2016; Wang 2014) are both important means to study major topics such as planet formation, black hole physics and dark energy in the universe. In order to further improve the level of science and technology, the construction of the China Array of Radio Telescopes (CHINA-ART) proposed in recent years can achieve leap-forward development of Chinese astronomical science in many fields such as astrometry and deep space navigation (Han 2011; Zhu et al. 2012; Lesovoi et al. 2014). With the development of science and technology, large radio telescopes are playing an increasingly important role.

Several large reflector telescopes have been built around the world. The Green Bank Telescope (Prestage et al. 2009) relies on an offset feed design with a 110 m$\times$100 m reflector, and its total self-weight is 7856 t. The German Effelsberg (Hachenberg et al. 1973) 100 m large aperture antenna, whose reflector adopts an umbrella back-up structure, has a total self-weight of 3200 t. To explore the domain of more distant stars, more large aperture radio telescopes require further development (Tang et al. 2003; James et al. 2019). For a fully-steerable radio telescope, the self-weight of the reflector is roughly proportional to the aperture, however due to effect of gravity generating a serious problem with deformation, the surface accuracy of the reflector will be seriously affected (Sun et al. 2016; Zhang et al. 2018; He et al. 2020). With further increase in the reflector aperture, this problem will become more and more serious, so the technical challenges of the reflector structure become more difficult to overcome (Li et al. 2020), and how to meet the performance requirements under the condition of reducing weight of the reflector becomes the technical bottleneck of the application (Li et al. 2017; Jin et al. 2006; Wang et al. 2020).

In the face of these pressing needs, this paper proposes a new mesh structure scheme for a large fully-steerable radio telescope reflector. Adopting this scheme for the reflector system can ensure the performance meets the requirements, significantly reduce the mass of the reflector and greatly reduce the system structure complexity, thus promoting the application and development of a large fully-steerable radio telescope.

2 DESIGN SCHEME FOR REFLECTOR

The purpose of this paper is to reduce the structural complexity and mass of the reflector significantly under the condition of satisfying the performance requirements through the innovative design of the reflector structure. In order to achieve the above purpose, the performance requirements of the reflector should be ensured first. For the radio telescope, the efficiency of the reflecting surface is one of the key performance requirements. According to the classical Ruze formula (Ruze 1952), the efficiency of the reflecting surface is directly related to the surface accuracy. The gain decline coefficient η_s is defined as

$$\eta_s = \frac{G}{G_0} = e^{-(\frac{4\pi\sigma}{\lambda})^2}. \quad (1)$$

Here the function G_0 is the antenna gain without profile error; G is the antenna gain with profile error; σ is the root mean square (RMS) of the reflecting surface; λ is the wavelength. As the ratio of the reflection surface profile error to the working wavelength gradually increases, the efficiency of the reflecting surface will decrease rapidly. For a large radio telescope, the desired accuracy is often very high to ensure the efficiency of the reflecting surface (Tang et al. 2020). With further increase in the reflector aperture, the influence of gravity deformation will become more and more serious, and the expected surface accuracy will also become increasingly difficult to ensure, so it is necessary to carry out a lightweight design for the reflector system.

In order to reduce the self-weight, the common method is to consider the material and structure. In terms of material, in order to meet the characteristics of lightweight and high reliability, commonly utilized engineering materials include steel, aluminum alloy or carbon fiber, as displayed in Table 1. Compared with a traditional aluminum alloy tube and steel tube, a carbon fiber tube has lighter weight, higher strength, smaller thermal expansion coefficient and excellent corrosion and radiation resistance. However, due to its high cost, carbon fiber material is currently difficult to implement in a wide range of applications.

This paper takes the representative Effelsberg antenna as the prototype, under the condition that the other structures except the reflector remain unchanged, and the research is carried out by replacing the umbrella back-up structure. Based on the previous experience with a deployable antenna and cable net structure (Rui et al. 2020, 2021; Zheng et al. 2019a,b, 2020, Patent pending), through

Table 1 Material Attribute

Material	Density ($\mathrm{kg\,m^{-3}}$)	Elastic modulus (Pa)	Poisson ratio
Steel	7.8×10^3	2.07×10^{11}	0.29
Aluminum alloy	2.7×10^3	7.17×10^{10}	0.33
Carbon fiber	1.8×10^3	2.35×10^{11}	0.3

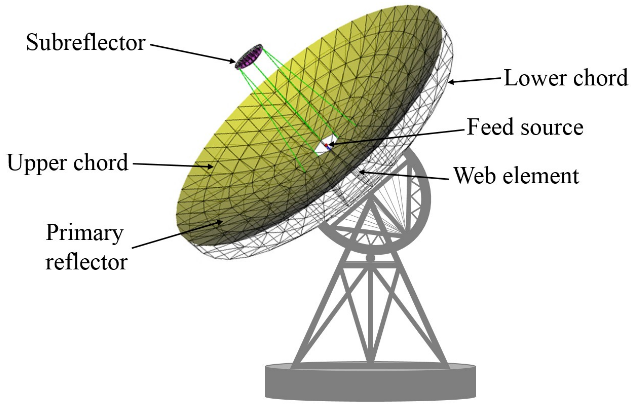

Fig. 1 Schematic diagram of a large fully-steerable radio telescope reflector system structure.

repeated analysis, comparison, modeling and attempts, we put forward a new reflector structure scheme for large radio telescopes. The system structure of the reflector mainly includes two parts: the back-up structure and the reflecting surface, as illustrated in Figure 1.

2.1 Reflector Composed of a Homogenized Mesh

In the reflector system structure featured in Figure 1, the main function of the primary reflector and subreflector is to reflect and concentrate electromagnetic waves, while the upper chord, lower chord and web elements in the back-up structure are used to support the corresponding reflecting surface through the truss structure. Although the traditional antennas of the Green Bank Telescope in the United States and Effelsberg in Germany can meet the requirements of precision through their complex back-up structures, their heavy reflectors make antennas expensive to build and consume serious power. Besides, with further increase in the reflector aperture, the technical difficulty will become higher, so the traditional scheme is difficult to apply in a radio telescope with larger aperture.

This paper is based on the stability provided by a planar triangle and space tetrahedron structure mechanism, and further proposes that the corresponding chords in the upper chord surface and lower chord surface are arranged in a quasi-geodesic mesh form composed of triangular mesh elements, which makes the whole back-up structure uniform, simple and symmetrical. At the same time, in order to strengthen the stability of the support between the

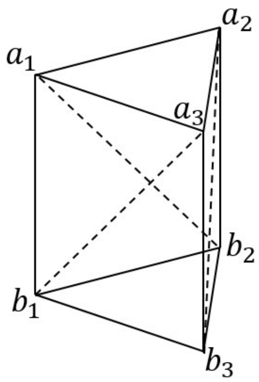

Fig. 2 Diagram of back-up structure unit.

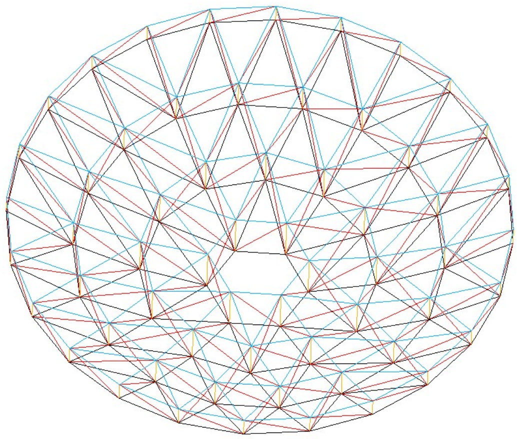

Fig. 3 Diagram of whole back-up structure.

upper chord surface and the lower chord surface, several web elements are set between the upper chord surface and the lower chord surface according to a regular quasi-tri-prism or tetrahedron. As a result, the reflector system not only ensures structural stability, but also minimizes the simplification of the back-up structure, thus reducing the self-weight of the reflector.

As depicted in Figure 2, we assume that a_1, a_2, a_3 are a set of adjacent upper chord nodes, and b_1, b_2, b_3 are a set of corresponding lower chord nodes, with two sets of nodes which are both connected by chords to form a structurally stable triangle structure. At the same time these two sets of nodes are connected with web elements in order to form a regular quasi-tri-prism like $\overline{a_1b_1}, \overline{a_2b_2}, \overline{a_3b_3}$ or tetrahedron like $\overline{a_1b_1}, \overline{a_2b_2}, \overline{a_3b_3}, \overline{a_1b_2}, \overline{a_2b_3}, \overline{a_3b_1}$. The integral truss structure, based on the above structural element forms, constitutes an integral uniform, ultra-light and stable back-up structure, and its simplified schematic diagram is displayed in Figure 3.

On this basis, we exploit the characteristics of a tree structure in nature as shown in Figure 4, and the biological principle of chord diameter, with a gradual change from inside to outside, is adopted for the quasi-tri-prism or tetrahedron elements which constitute the back-up structure. Therefore, the self-weight of the back-up structure can be reduced to the maximum extent under the premise of ensuring structural stability. The gradual chord diameter is defined as

Fig. 4 Diagram of tree structure.

$$g_w = C^{w-1} g_0 \,. \tag{2}$$

Here the function g_w is the chord diameter of group w; C is the gradient coefficient; g_0 is the largest diameter; $w = 1, 2, \ldots, n$; n is the number of reflector radial rings.

The mesh structure scheme of the reflector system based on these above key points can ensure that the reflector meets the basic performance while at the same time greatly reducing the self-weight and structural complexity, further optimizing the whole system and yielding high performance. The basic structure is described below.

2.2 Lower Chord Surface

The lower chord surface is composed of a lower chord inner ring frame, lower chord outer ring frame, main lower chord and secondary lower chord. The main lower chords are radially distributed between the lower chord inner ring frame and the lower chord outer ring frame. According to the form of a quasi-geodesic grid, the secondary lower chords are evenly distributed in the space area formed by the lower chord inner ring frame, the lower chord outer ring frame and the adjacent main lower chords. The whole lower chord surface is composed of two parts: the parabolic truss structure and the bottom platform truss structure.

As shown in Figure 5, all the lower chord node positions are distributed in the form of a quasi-geodesic grid. The coordinates of each node can be calculated as

$$\begin{cases} X_{tjk} = \frac{(D-D_k)t+nD_k}{2n} \sin \frac{2\pi(\frac{k}{t}+j)}{d} \\ Y_{tjk} = \frac{(D-D_k)t+nD_k}{2n} \cos \frac{2\pi(\frac{k}{t}+j)}{d} \\ Z_{tjk} = \begin{cases} B_p & t \leq N \\ B_p + \frac{X_{tjk}^2+Y_{tjk}^2-U_{tjk}^2}{4f_x} & t > N \end{cases} \end{cases} . \tag{3}$$

Here the function B_p is height of the lower chord inner ring frame; N is the number of bottom platform truss

Table 2 Optimization Results of Reflector Surface Accuracy

Objective function	Steel			Aluminum alloy			Carbon fiber		
	Zenith	45°	Horizon	Zenith	45°	Horizon	Zenith	45°	Horizon
Maximum deformation (mm)	9.17	27.55	30.43	11.28	34.70	38.34	6.49	15.38	15.45
RMS of absolute displacement error (mm)	6.63	13.01	17.16	8.41	16.17	21.26	4.15	6.48	8.16
RMS of normal error (mm)	0.56	0.52	0.49	0.79	0.69	0.58	0.16	0.17	0.18
RMS of half optical path difference (mm)	0.52	0.48	0.44	0.73	0.64	0.52	0.14	0.15	0.16

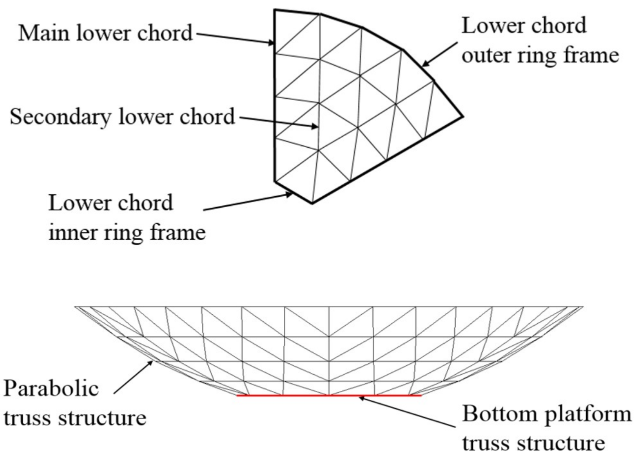

Fig. 5 Diagram of lower chord surface structure. (a) Structure composition of chord; (b) Integral truss structure.

Table 3 Optimization Results of Reflector Mass

Objective function	Steel	Aluminum alloy	Carbon fiber
Upper chord (t)	66.89	24.13	32.09
Web element (t)	360.55	201.21	70.48
Lower chord (t)	145.80	59.81	20.24
Total mass (t)	698.17	379.52	203.96
Surface density (kg m^{-2})	61.73	33.56	18.03

structure radial rings; d is the circumferential fraction of the reflector; D is the reflector diameter; D_k is the feed diameter; $t = 1, 2, \ldots, n$; $j = 1, 2, \ldots, d$; $k = 1, 2, \ldots, t$; $f_x = \frac{fD^2}{D^2+16f(B_m-B_p)}$; B_m is height of the lower chord outer ring frame; f is the focal length of the reflector; $U_{tjk} = \frac{(D-D_k)N+nD_k}{2n}$.

2.3 Upper Chord Surface

The upper chord surface has basically the same structure as the lower chord surface, including a parabolic truss structure composed of the upper chord inner ring frame, the upper chord outer ring frame, the main upper chords and the secondary upper chords. Each position of an upper chord node is provided with an actuator for adjusting the position of the panel, and each actuator can control six adjacent panel corners. The position coordinates of the upper chord nodes can be obtained through calculation.

$$\begin{cases} \grave{X}_{tjk} = \frac{(D-D_k)t+nD_k}{2n} \sin\frac{2\pi(\frac{k}{t}+j)}{d} \\ \grave{Y}_{tjk} = \frac{(D-D_k)t+nD_k}{2n} \cos\frac{2\pi(\frac{k}{t}+j)}{d} \\ \grave{Z}_{tjk} = \frac{\grave{X}_{tjk}{}^2+\grave{Y}_{tjk}{}^2}{4f} \end{cases} . \tag{4}$$

2.4 Reflecting Surface

The reflecting surface consists of two parts: the primary reflector and the subreflector. Since the self-weight and precision of the primary reflector are much greater than those of the subreflector, this paper mainly focuses on the structure of the primary reflector here.

In a large radio telescope reflector, the primary reflector is usually composed of several light metal plates joined together. Regarding different linking schemes, the shape of the light metal plates can be triangular or trapezoidal, as diagrammed in Figure 6. The trapezoidal panels can significantly reduce the quantity and cost of molds because of the same panel shape in each ring. The triangular panels can provide higher surface accuracy due to their almost identical panel area and being relatively easy to control, but at the same time, the number of units and cost will also increase. In the following research, we can choose the required panel shape of the primary reflector according to task requirements.

3 SIMULATION AND OPTIMIZATION OF REFLECTOR

In this paper, the new reflector mesh structure scheme for a large fully-steerable radio telescope is briefly discussed. In practice, because most radio telescopes need to be exposed to the natural environment for a long time, under the influence of gravity, wind, temperature and other different loads, the reflector structure will deform, resulting in the deterioration of its electrical performance (Yang et al. 2011). Among them, gravity deformation has always been the problem that most concerns researchers, and this paper will analyze the primary reflector whose surface accuracy changes with pitch angle under the influence of gravity deformation. At present, researchers usually rely on finite element analysis to obtain the simulation model of the reflector in the design stage (Wang et al. 2017). Therefore, in order to verify the rationality and feasibility of this scheme, the reflector in the scheme is applied to the mathematical simulation analysis for verification. In this

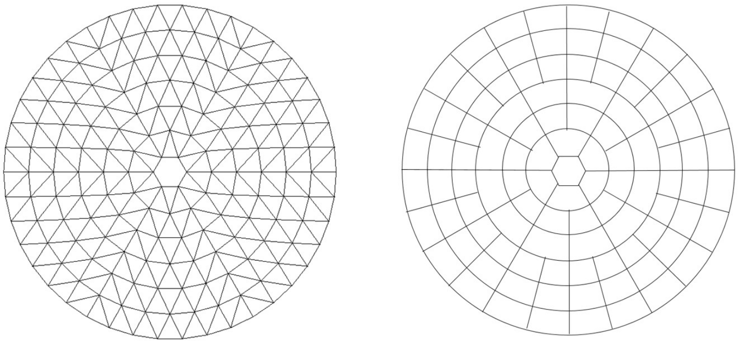

Fig. 6 Diagram of primary reflector structure. (a) Triangular panel; (b) Trapezoidal panel.

Table 4 Results of Comparing Model Surface Accuracy

Objective function	Steel			Aluminum alloy			Carbon fiber		
	Zenith	45°	Horizon	Zenith	45°	Horizon	Zenith	45°	Horizon
Maximum deformation (mm)	6.86	16.39	16.45	7.78	20.08	20.78	5.53	11.29	10.49
RMS of absolute displacement error (mm)	4.81	6.17	7.29	5.57	7.78	9.48	3.30	3.85	4.34
RMS of normal error (mm)	0.55	0.47	0.37	0.77	0.74	0.70	0.19	0.19	0.20
RMS of half optical path difference (mm)	0.51	0.43	0.33	0.71	0.68	0.64	0.18	0.17	0.17

paper, a radio telescope reflector with an aperture of 120 m is taken as an example.

In the simulation, in order to better meet the design requirements of the reflector system, it is necessary to optimize the preliminary system scheme (Duan 1998). Parameters to be optimized include element size optimization, number of radial rings and spatial position. The element size optimization includes diameter optimization and wall thickness optimization for each element section. With the increase in diameter and wall thickness, the stiffness of the corresponding element will increase, but at the same time, the influence of gravity will also increase. Optimizing the number of radial rings and spatial position for the whole back-up structure is important, since the number of radial rings in the upper chord surface and the lower chord surface as well as the relative position relationship between the two surfaces will have a direct impact on the structural stability. How to choose the appropriate scheme within a reasonable range is the problem to be solved in this optimization.

The objective of this optimization is to reduce the mass of the reflector system as much as possible while ensuring that the reflector system can meet the accuracy requirements, and select the appropriate scheme through comprehensive analysis. In the calculation of surface accuracy, the common method is to adopt a homological design and compensate the position of reflecting surface or feed source through the driving system. Therefore, the influence of these rigid bodies' translation, rotation and focal length change on the electrical properties should be removed when calculating surface accuracy. Therefore, the geometric deformation parameters of the best-fit paraboloid can be determined according to the least squares method, and then the RMS of half the optical path difference and normal error of deformed nodes can be calculated. Referring to the relevant parameters of the Effelsberg antenna in Germany, the constraint conditions of this optimization are that the surface accuracy of the distorted reflector relative to the best-fit paraboloid ACC is less than 1 mm and the total mass of the reflector $TMASS$ is less than 750 t. The objective function is to minimize the surface accuracy and total mass. The optimized mathematical model is

$$FindX = \begin{bmatrix} S_w & S_n & S_f & Q_w & Q_n & Q_f & P_w \\ P_n & P_f & n & N & B_p & B_m & C \end{bmatrix}^T ,$$

$$Min: \begin{cases} TMASS = \sum_{\tau=1}^{2} \rho_\tau v_\tau \\ ACC = \sqrt{\dfrac{\sum_{\gamma=1}^{m} \delta_\gamma^2 q_\gamma a_\gamma}{\sum_{\gamma=1}^{m} q_\gamma a_\gamma}} \end{cases} ,$$

$$S.t. \begin{cases} TMASS \leq 750\,\mathrm{t} \\ ACC \leq 0.001\,\mathrm{m} \end{cases} .$$

Here the functions S_w, S_n and S_f are, respectively, the diameter, wall thickness and diameter ratio of main chord and secondary chord in the upper chord element section; Q_w, Q_n and Q_f are, respectively, the diameter, wall thickness and diameter ratio of vertical member and diagonal member in the web element section; P_w, P_n and P_f are, respectively, the diameter, wall thickness and diameter ratio of main chord and secondary chord in the lower chord element section; ρ_τ and v_τ are, respectively, the density and volume of the τth material in the reflector;

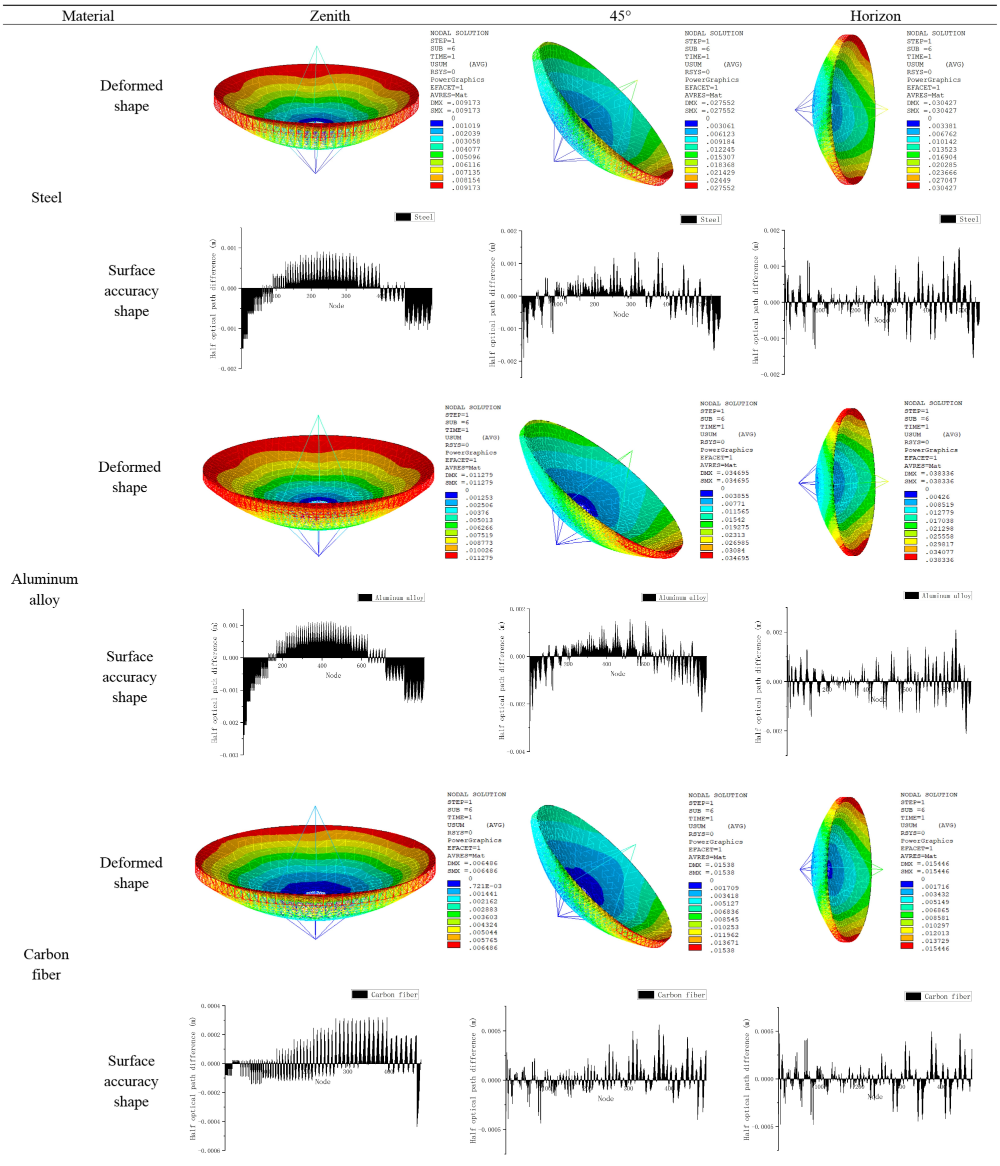

Fig. 7 Simulation results of reflector.

m is the number of upper chord nodes; δ_γ is half optical path difference of the γth node; q_γ is irradiation coefficient of the γth node; a_γ is influential area of the γth node.

In this paper, the reflector models of steel, aluminum alloy and carbon fiber back-up structure are optimized separately. According to the optimization results, the reflector simulation models under three position states are obtained, as depicted in Figure 7. By observing the simulation models in Figure 7, it can be concluded that the nodes with large deformation in each model are mainly distributed at the position of the reflector's outer boundary. Since the nodes here are more susceptible to gravity, the deformation effect is also greater. In addition, with the change in pitch angle, the deformation error and surface accuracy will also change gradually. When the reflector models are in the critical zenith or horizon position state, the surface accuracy is the worst, and the deformation effect is the most serious. According to the normal operation of radio telescopes, the reflector is rarely in these two critical states, so the larger deformation in these states does not affect the overall accuracy too much.

The optimization results of reflector surface accuracy can be obtained through calculation, and accuracy of the results is described from four aspects in this paper: for deformed nodes relative to an ideal paraboloid, we mainly consider the maximum deformation and the RMS of absolute displacement error. For deformed nodes relative to best-fit paraboloid, we mainly consider the RMS of half optical path difference and normal error, as expressed in Table 2. The carbon fiber model has the

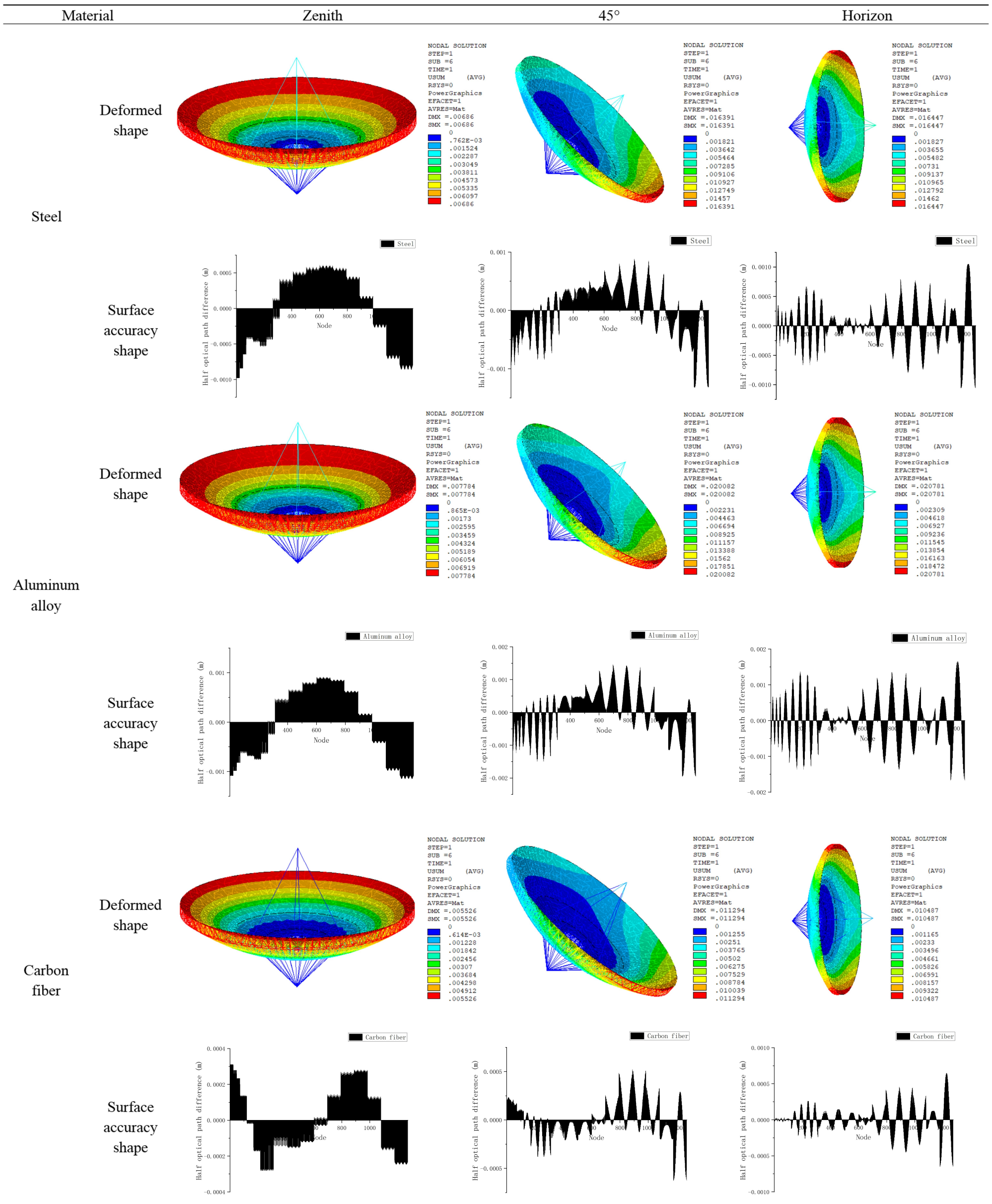

Fig. 8 Simulation results of comparison model.

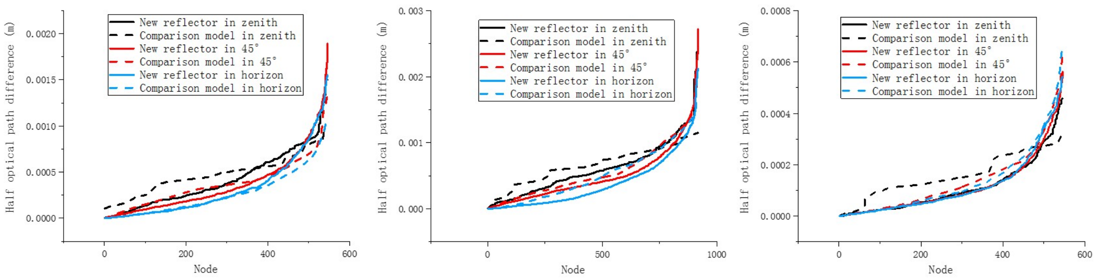

Fig. 9 Comparison graph of surface accuracy. (a) Steel; (b) Aluminum alloy; (c) Carbon fiber.

best performance, while the aluminum alloy model has the weakest performance. According to the data in Table 2, the reflectors of steel, aluminum alloy and carbon fiber can meet the working requirements of surface accuracy within 1 mm under different positions.

The mass optimization results of the reflector are displayed in Table 3. It can be seen from observation that the total mass of the carbon fiber model is the lowest, and that of the steel model is the highest. For the back-up structure, the lower chords and web elements need to support the large reflector, so in order to ensure the stability of the whole structure, the sum of their masses is relatively high; the upper chords are designed to minimize the influence of gravity, so their total mass is relatively low, and the above conclusions are consistent with the results described in Table 3. According to the data, the self-weight of the steel, aluminum alloy and carbon fiber reflectors can be controlled within 750 t.

Based on the above analysis, it can be concluded that due to uniform, simple and stable characteristics of the back-up structure, the new reflector can ensure that surface density is relatively low while meeting the accuracy requirements. The self-weight of the steel, aluminum alloy and carbon fiber reflectors can be controlled within 750 t, and the surface accuracy can be within 1 mm. The steel material has a high elastic modulus, so the reflector can maintain relatively high stability. Aluminum alloy material has a lower density, so the reflector has a lighter mass. Carbon fiber material has excellent material properties, so the reflector has the most ideal performance among the above materials, but due to its high cost, it is not currently suitable for all applications.

4 CONTRASTING ARGUMENT ON REFLECTOR

Among the existing radio telescopes, the Effelsberg 100 m antenna from Germany built in 1969 is a representative large fully-steerable radio telescope with excellent performance. Since the Effelsberg is the most similar reflector structure to the scheme proposed in this paper, the main difference between the two designs is that the new reflector exemplified above is based on the back-up structure in the form of a quasi-geodesic grid and tetrahedron, while the Effelsberg adopts a back-up structure based on a radial isosceles trapezoidal grid and umbrella support. Therefore, we further argue the rationality of the scheme by comparing and analyzing the simulation results. After multi-objective optimization under the same optimization conditions as the new reflector, the simulation results of the comparison model based on the Effelsberg antenna are depicted in Figure 8. Since this comparative analysis mainly focuses on the mesh structure scheme of the reflector, the comparison model does not consider the influence caused by chassis deformation, manufacturing error or other factors. In the same way, the self-weight of elevation main drive gear, chassis and other structures is also not considered, so although the simulation results are slightly different from the actual results, they are basically consistent.

Table 5 Results of Comparison Model Mass

Objective function	Steel	Aluminum alloy	Carbon fiber
Upper chord (t)	114.91	39.78	26.52
Web element (t)	479.47	165.97	110.65
Lower chord (t)	226.32	78.34	52.23
Total mass (t)	1030.49	386.54	272.90
Surface density (kg m^{-2})	131.21	49.22	34.75

As can be seen from the simulation results featured in Figure 8, the reflector structure of the Effelsberg antenna can meet the basic performance requirements of the antenna system in different positions. The surface accuracy and mass results are listed in Table 4 and Table 5 respectively. The traditional steel reflector can ensure that the surface accuracy is within 1 mm, and the total mass is about 1030 t, which is basically consistent with the actual results. Assuming that aluminum alloy or carbon fiber is utilized as the back-up structure material in this comparison model, although the aluminum alloy model has lighter mass than the steel model, the surface accuracy is slightly decreased. Relatively, the carbon fiber model still has the best performance, which is consistent with the simulation results of the new reflector in this paper.

In order to better verify the rationality of the new reflector structure scheme proposed in this paper, the new reflector is compared with the surface accuracy and mass results of the comparison model, as shown in Figure 9 and Figure 10 respectively. Figure 9 is the general trend comparison graph of each upper chord node surface accuracy in order from lowest to highest absolute value. By comparing the steel model, the general trend in surface accuracy of the new reflector is slightly lower than that of the comparison model and the maximum deviation is within 1 mm. In the aluminum alloy model, the general trend in surface accuracy of the two models is basically the same. In the carbon fiber model, the surface accuracy general trend of the new reflector is slightly higher. According to the above results, it can be concluded that the general trend in surface accuracy of the two reflectors is slightly different, but both can meet the accuracy requirements of the reflector system.

In terms of mass, we can compare the data in Table 3 and Table 5. Due to the smaller aperture of the comparison model, the mass of some beam elements is slightly lower, but overall, the surface density of the new reflector is much less than the comparison model incorporating the same

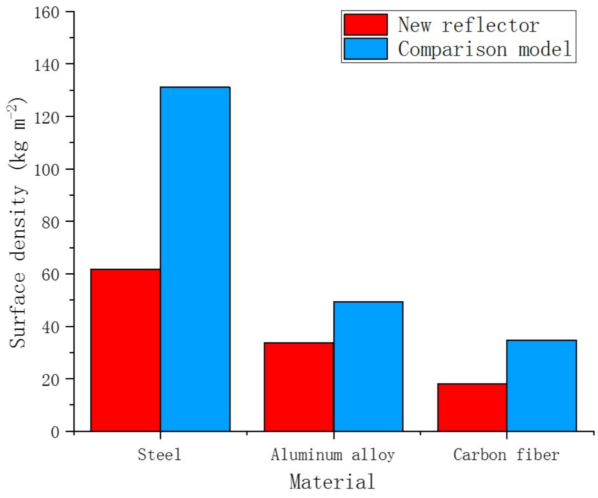

Fig. 10 Comparison graph of surface density.

material. Figure 10 shows the surface density comparison of the two reflectors It can be ascertained that the self-weight results of different back-up structures are also different. By comparing the comparison model with the new reflector of the same material, the self-weight of the new reflector can be reduced by 53.0%, 31.8% and 48.1% when using steel, aluminum alloy and carbon fiber respectively. Among them, steel as a traditional material has the most prominent self-weight reduction effect. If the self-weight of a steel comparison model is reduced to less than 750 t, the corresponding surface accuracy can only be maintained at about 1.1 mm. Compared with the accuracy results of the new reflector, the accuracy of the comparison model will be much lower under the condition of basically the same surface density. According to the above results, it can be concluded that the new reflector in this paper can achieve the expected goal of significantly reducing the structural complexity and self-weight through the homogenized mesh structure.

5 CONCLUSIONS

The aim of this paper is to reduce the self-weight and structural complexity of a large fully-steerable radio telescope under the condition of satisfying the performance requirements. Based on the planar triangle and space tetrahedron structure stability mechanism, the new reflector structure in the form of the quasi-geodesic grid and regular quasi-tri-prism or tetrahedron element is proposed in this paper. The mesh structure has the characteristics of being simple, stable, homogeneous and can effectively solve the technical problems raised in the above objectives.

In this paper, the radio telescope reflector with an aperture of 120 m is simulated and the rationality of the scheme is verified by a contrasting argument. Compared with the traditional reflector structure scheme, the new reflector structure scheme proposed in this paper has the advantage of being lightweight with simple structure, which can achieve the expected goal of significantly reducing the self-weight and structural complexity under the condition that the performance meets the requirements. For QTT, the world's largest fully-steerable reflector antenna, to be built in Xinjiang, the planned surface accuracy is 0.3 mm under the influence of self-weight, the mass of the reflector is about 3000 t and the surface density is about 316 kg m . If the reflector structure proposed in this paper is adopted, the mass of the reflector can be further greatly reduced and the performance of the antenna can be effectively improved. In future research, a general active surface can also be employed for active adjustment to ensure that the surface accuracy can meet the requirements. At the same time, the idea for structural design and method proposed in this paper can also be extended to further increase the aperture of the radio telescope, which provides guidance for a new reflector structural design in future research on a large fully-steerable radio telescope.

Acknowledgements This work was partially supported by the National Natural Science Foundation of China (Grant No. 50975217).

References

Cheng, J. Q. 2009, The Principles of Astronomical Telescope Design (New York: Springer)https://doi.org/10.1007/b105475

Duan, B. Y. 1998, Antenna Structural Analysis, Optimization and Measurement (in Chinese) (Xidian Univ. Press)

Gan, H. Q., & Jin, C. J. 2010, RAA (Research in Astronomy and Astrophysics), 10, 797

Hachenberg, O., Grahl, B. H., & Wielebinski, R. 1973, IEEE Proceedings, 61, 1288

Han, J. L. 2011, Science(Shanghai), 63, 4 (in Chinese) 10.3969/j.issn.0368-6396.2011.01.002

Hao, L. F., Wang, M., & Yang, J. 2010, RAA (Research in Astronomy and Astrophysics), 10, 805

He, F. L., Xu, Q., Wang, N., & Zhu, C. H. 2020, RAA (Research in Astronomy and Astrophysics), 20, 82

James, C. W., Bray, J. D., & Ekers, R. D. 2019, RAA (Research in Astronomy and Astrophysics), 19, 25

Jin, C., Cao, Y., Chen, H., et al. 2006, ChJAA (Chin. J. Astron. Astrophys.), 6S, 319

Lesovoi, S. V., Altyntsev, A. T., Ivanov, E. F., & Gubin, A. V. 2014, RAA (Research in Astronomy and Astrophysics), 14, 864

Li, D., Gajjar, V., Wang, P., et al. 2020, RAA (Research in Astronomy and Astrophysics), 20, 133

Li, N., Li, P., Wu, J., & Duan, B. Y. 2017, RAA (Research in Astronomy and Astrophysics), 17, 15
Nan, R. D. 2005, Science in China Series G-Physics, Mechanics & Astronomy (in Chinese), 35, 449, https://doi.org/10.1360/2005-35-5-449
Prestage, R. M., Constantikes, K. T., Hunter, T. R., et al. 2009, IEEE Proceedings, 97, 1382
Rui, X., Zheng, F., & Yan, L. D. 2021, Applied Thermal Engineering, 186, 116496, https://doi.org/10.1016/j.applthermaleng.2020.116496
Rui, X., Zheng, F., Zheng, T., Ji, X., & Wu, T. 2020, Energy Science and Engineering, 8, 181, https://doi.org/10.1002/ese3.519
Ruze, J. 1952, Il Nuovo Cimento, 9, 364
Sun, Z. X., Wang, J. Q., & Chen, L. 2016, RAA (Research in Astronomy and Astrophysics), 16, 119
Tang, W., Zhu, L. C., & Wang, Q. M. 2020, RAA (Research in Astronomy and Astrophysics), 20, 120
Tang, X. Q., Wang, J. S., & Wang, Q. M. 2003, ChJAA (Chin. J. Astron. Astrophys.), 3, 478
Wang, C. S., Xiao, L., Wang, W., et al. 2017, RAA (Research in Astronomy and Astrophysics), 17, 043
Wang, J. Q., Zhao, R. B., Jiang, Y. C., et al. 2020, RAA (Research in Astronomy and Astrophysics), 20, 009
Wang, N. 2014, Scientia Sinica Physica, Mechanica & Astronomica (in Chinese), 44, 783
Xu, Q., & Wang, N. 2016, in Ground-Based and Airborne Telescopes VI, SPIE, 9906, 99065L
Yang, D. H., Okoh, D., Zhou, G. H., et al. 2011, RAA (Research in Astronomy and Astrophysics), 11, 725
Zhang, H. Y., Wu, M. C., Yue, Y. L., Gan, H. Q.and Hu, H., & Huang, S. J. 2018, RAA (Research in Astronomy and Astrophysics), 18, 048
Zhang, J. S., Li, D., Wang, J. Z., Zhu, Q. F., & Li, J. 2019, RAA (Research in Astronomy and Astrophysics), 19, 022
Zheng, F., Yan, L. D., Chen, M., & Rui, X. 2020, Patent Pending, Reflector Antenna Based on a Three-extensible-rod Tracker and Quasi-geodesic Grid Structure (in Chinese), Patent
Zheng, T., Zheng, F., Rui, X., et al. 2019a, Solar Energy, 193, 335
Zheng, T., Zheng, F., Rui, X., & Yan, L. D. 2019b, International Journal of Antennas and Propagation, 2019, 3980947, https://doi.org/10.1155/2019/3980947
Zheng, T., Zheng, F., Rui, X., et al. 2020, Acta astronautica, 169, 1, https://doi.org/10.1016/j.actaastro.2019.12.021
Zhu, X. Y., Zhang, X. Z., Zhang, H. B., et al. 2012, RAA (Research in Astronomy and Astrophysics), 12, 857